ELSEVIER

Tectonophysics 337 (2001) 99–116

TECTONOPHYSICS

www.elsevier.com/locate/tecto

Characteristics of the seismic quiescence and activation patterns before the $M = 7.2$ Kobe earthquake, January 17, 1995

Qinghua Huang[a,*], Guennadi A. Sobolev[b], Toshiyasu Nagao[c]

[a]*International Frontier Research Group on Earthquakes, RIKEN, The Institute of Physical and Chemical Research, c/o Tokai University, 3-20-1, Orido, Shimizu, Shizuoka 424-8610, Japan*

[b]*United Institute of Physics of the Earth, Russian Academy of Sciences, 10, B. Gruzinskaya, Moscow 123810, Russian Federation*

[c]*Earthquake Prediction Research Center, Tokai University, 3-20-1, Orido, Shimizu, Shizuoka 424-8610, Japan*

Received 31 July 2000; accepted 30 March 2001

Abstract

We investigated the characteristics of the seismicity changes associated with the $M = 7.2$ Kobe (Japan) earthquake, January 17, 1995 by applying the Region–Time–Length (RTL) algorithm to the earthquake catalog of the Japan meteorological agency (JMA). The weighted coefficients associated with all three parameters (time, place and magnitude) of earthquakes are taken into account in this algorithm. The JMA catalog after eliminating aftershocks is complete for events with $M \geq 3$ in most parts of the Japanese islands during 1977–1995. The RTL parameters at the epicenter indicated that a seismic quiescence (a decrease of seismicity compared to the preceding background rate) started in 1993 and reached its bottom in May 1994. An activation stage (an increase of seismicity compared to the preceding background rate) with duration of about seven months followed. Our detailed investigations indicated that the RTL anomaly during 1993–1994 would not be an artificial effect due to the influence of the changes of some threshold parameters or the changes of the JMA seismological network. The spatial distribution of quiescence during 1993–1994 revealed a significant anomaly in a broad region around the epicenter of the Kobe earthquake. Following the quiescence stage, an activation zone, which was in order of the rupture length, was obtained around the epicenter during May–December 1994. The evolutions of spatial distributions of seismic quiescence and activation suggested that above anomalies around the epicentral zone would have reasonable correlation with the preparation of the Kobe earthquake. The primary characteristics of the seismicity changes prior to the Kobe earthquake are similar to those obtained for other large earthquakes in Kamchatka and Hokkaido. Therefore, the seismicity changes revealed in this study may give better understanding of the seismogenic process of the Kobe earthquake and provide useful information for seismic risk estimation.

Keywords: seismicity; quiescence; activation; precursor; Kobe earthquake

1. Introduction

A strong earthquake with $M = 7.2$ struck the Kobe–Osaka region in central Japan on January 17, 1995. More than 6400 people died during this event, which was named the 'Kobe earthquake'. Other popular names of this event are the 'Great Hanshin earthquake' and the 'Southern Hyogo Prefecture earthquake'. There were almost no warnings before this shock, except a seismic gap mentioned by Ishikawa (1990). Therefore, a close investigation on the seismicity changes associated with the Kobe

* Corresponding author. Tel.: +81-543-36-0591; fax: +81-543-36-0920.

E-mail address: huang@iord.u-tokai.ac.jp (Q. Huang).

0040-1951/01/$ - see front matter
PII: S0040-1951(01)00073-7

earthquake is important for understanding the nature of the seismo-tectonics of this region and the preparation of strong earthquakes.

Seismicity changes play an important role in intermediate-term earthquake prediction. Among all seismicity changes, seismic quiescence, which is defined as a decrease of mean seismicity compared to the preceding background rate in and around focal areas, may be one of the most promising intermediate-term precursors and has received much attention (Mogi, 1979; Habermann, 1988; Wyss and Habermann, 1988; Ishikawa, 1990; Wiemer and Wyss, 1994). Several methods, which can reveal the precursory seismic quiescence based on earthquake catalogs, were tested in various studies on earthquake prediction and risk estimation (Wyss and Habermann, 1988; Keilis-Borok and Kossobokov, 1990; Kossobokov and Keilis-Borok, 1990). However, the primary attention was concentrated on seismic quiescence (Wyss et al., 1984; Taylor et al., 1991; Wiemer and Wyss, 1994; Takanami et al., 1996; Katsumata and Kasahara, 1999). Few of these approaches dealt with the seismic activation, which is defined as an increase of mean seismicity compared to the preceding background rate in and around focal areas.

The physics of the earthquake source is, in essence, the physics of the rupture of material due to tectonic stresses. The experimental data of fracture mechanics allow creating a qualitative picture of the earthquake preparation process. The macrofracture of statistically heterogeneous material is caused by the increase of number of smaller size fractures. Macrofracture (developing of the main fault) is the result of the avalanche-like growth and instability, which occurs on reaching a certain critical density of fractures. The main ideas of this qualitative model were discussed in Mjachkin et al. (1975) and Sobolev (1995).

If this process leads to the earthquake then it is unstable. Unstable deformation (and fracturing) is restricted to a narrow zone of future macrofracture. This stage has been observed in laboratory experiments (Mogi, 1968; Scholz, 1968). Formation of the main fault results in the decrease of stress level in the surrounding volume; as a result, the growth of new fractures outside of macrofracture zone is decreased.

Two main physical (seismological) sequences follow from this approach: (1) the appearance of seismic quiescence in relatively large volume around of future earthquake fault; (2) increasing of seismic activity near the future earthquake fault.

The modern critical point hypothesis (self-organized seismic criticality), which includes the interaction of different size faults and accelerating seismicity during large earthquake preparation, does not contradict to above mentioned conceptions (Varnes, 1989; Sornette and Sammis, 1995; Bowman et al., 1998).

The recently developed technique can investigate the characteristics of seismicity changes, from physical ideas of the stages of seismic quiescence and activation (Sobolev and Tyupkin, 1997). This technique is called as the Region–Time–Length (RTL) algorithm, where RTL is a parameter of the combination of three functions associated with distance, time and rupture length, respectively. All three parameters (time, place and magnitude) of earthquakes are taken into account with weighted coefficients in the RTL algorithm. We will introduce this algorithm in Section 2. This technique was tested using the earthquake catalog of Kamchatka, Russia (Sobolev and Tyupkin, 1997, 1999) and the earthquake catalog of the Japan meteorological agency (JMA) (Huang and Sobolev, 2001). The results indicated that the strong earthquakes with magnitude $M > 7$ in Kamchatka and the $M = 6.8$ Nemuro Peninsula earthquake in Hokkaido had been preceded by seismic quiescence and activation patterns. The seismic quiescence stages started 1.5–3.5 years before the mainshock and lasted 1–2.5 years. The subsequent stages of seismic activation had a duration varying from 6 months to 1.5 years. The linear dimension of the quiescence zone was several times larger than the rupture length of the mainshock, while the activation zone was in order of several tens of kilometers, comparable to the rupture length.

In this study, we apply the RTL algorithm to the investigation of the seismicity changes associated with the $M = 7.2$ Kobe earthquake, January 17, 1995, by using the JMA earthquake catalog. First, we eliminate aftershocks from the original JMA catalog and estimate the completeness of this catalog. Next, we discuss the temporal variation of the seismicity changes and the spatial distribution of the seismic quiescence associated with this event using the RTL algorithm. Finally, we evaluate the spatial distribution

of the seismic activation using another independent algorithm, which takes the effective rupture area into account and is to be introduced in Section 2. Because seismicity changes may be caused either by the real changes associated with preparations of earthquakes or by the man-made changes due to the changes of seismological networks (Habermann, 1987, 1991), we also evaluate the data quality and explain the anomalies that are revealed from the RTL algorithm.

2. Methods

In order to invesitgate the evolution characteristics of the seismic quiescence and activation patterns, we eliminate aftershocks from the JMA catalog using the algorithm developed by Molchan and Dmitrieva (1991). Because earthquakes may not be reported homogeneously due to the inhomogeneous distribution of seismic stations in Japan, an island country, we also estimate the completeness of the JMA catalog based on the power law of frequency-magnitude before applying the RTL algorithm (Smirnov, 1998). We will introduce briefly the principles of aftershock elimination and completeness analysis in Section 3.

2.1. RTL algorithm

The basic assumption of the RTL algorithm is to allow a weighted coefficient of each event to the investigated earthquake at the position of (x, y, z). The weight of an event is greater when it is closer to the epicenter (x, y, z) and/or the occurrence time of the earthquake in question. Therefore, the predictive parameter RTL can be calculated by the combination of following three functions: epicentral distance, $R(x, y, z, t)$, time, $T(x, y, z, t)$ and rupture length, $L(x, y, z, t)$, where t is the analyzed time.

In the RTL algorithm, the above three functions are defined as

$$R(x,y,z,t) = \left[\sum_{i=1}^{n} \exp\left(-\frac{r_i}{r_0}\right)\right] - R_{\mathrm{tr}}(x,y,z,t), \qquad (1)$$

$$T(x,y,z,t) = \left[\sum_{i=1}^{n} \exp\left(-\frac{t-t_i}{t_0}\right)\right] - T_{\mathrm{tr}}(x,y,z,t)$$

$$L(x,y,z,t) = \left[\sum_{i=1}^{n} \left(\frac{l_i}{r_i}\right)\right] - L_{\mathrm{tr}}(x,y,z,t)$$

where l_i is the rupture dimension and t_i is the occurrence time of the ith earthquake; r_i is the distance from the position of (x, y, z) to the epicenter of the ith event; n is the number of events with their three parameters satisfying some criteria, e.g. $M_i \geq M_{\min}$ (M_i is the magnitude of the ith earthquake and $M_{\min}$ is the cut-off magnitude ensuring the completeness of the earthquake catalog), $r_i \leq R_{\max} = 2r_0$ and $(t - t_i) \leq T_{\max} = 2t_0$ (r_0 and t_0 are characteristic distance and time-span), $d_i \leq d_0$ (d_i is the focal depth of the ith earthquake and d_0 is the cut-off depth); $R_{\mathrm{tr}}(x, y, z, t)$, $T_{\mathrm{tr}}(x, y, z, t)$ and $L_{\mathrm{tr}}(x, y, z, t)$ are the trends (background values) of $R(x, y, z, t)$, $T(x, y, z, t)$ and $L(x, y, z, t)$, respectively.

One can see from Eq. (1) that $R(x, y, z, t)$, $T(x, y, z, t)$ and $L(x, y, z, t)$ are three dimensionless functions. They are further normalized by their standard deviations, σ_R, σ_T, and σ_L, respectively. The product of the above three functions is calculated as the RTL parameter, which describes the deviation from the background level of seismicity and is in units of the standard deviation, $\sigma = \sigma_R \sigma_T \sigma_L$. A decrease of RTL means a decrease of seismicity compared to the background rate around the investigated place, i.e. a decrease of RTL represents a seismic quiescence. A recovery stage from the quiescence to the background level can be considered as an activation stage of seismicity.

In this study, the temporal variation of the RTL curve is obtained by changing the calculated time, t in Eq. (1) at a step of 10 days. Because the RTL value at a certain time is calculated based on the earthquakes in the time window $[(t - T_{\max}), t]$, we cannot calculate the RTL value at the time $t < T_{\max}$. Namely, if the calculated period of background is T_{bk}, we can obtain the RTL curve only in the time interval $(T_{\mathrm{bk}} - T_{\max})$ (see Fig. 1).

The rupture dimension, l_i, is given by an empirical relation with the magnitude, M_i (Kasahara, 1981),

$$\log l_i(\mathrm{km}) = 0.5M_i - 1.8 \qquad (2)$$

The rupture length of the $M = 7.2$ Kobe earthquake is several tens of kilometers. After taking into account the reports of seismic quiescence around the rupture zone and our previous experiences in Kamchatka and

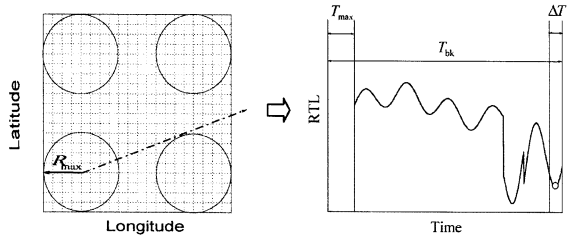

Fig. 1. A sketch description of calculating spatial distribution of seismic quiescence. ΔT and T_{bk} are the investigated interval and the interval for background calculation, respectively. R_{max} and T_{max} are the threshold values of distance and time-span, which satisfy $R_{max} = 2r_0$ and $T_{max} = 2t_0$ (r_0 and t_0 are characteristic distance and time-span). At each place, we can obtain an RTL-curve in interval ($T_{bk} - T_{max}$). We choose the minimum RTL value in interval ΔT (marked by a hollow circle) as an index of seismic quiescence at this place. We can obtain the quiescence map by changing the calculated place and repeating this procedure.

Hokkaido (Sobolev and Tyupkin, 1997, 1999; Huang and Sobolev, 2001), we assumed the characteristic distance, $r_0 = 50$ km, i.e. the threshold distance, $R_{max} = 2r_0 = 100$ km. We also assumed the characteristic time-span, $t_0 = 1$ year, i.e. the threshold time-span, $T_{max} = 2t_0 = 2$ years, based on the facts that duration of seismic quiescence is generally in order of one year and our previous experiences (Sobolev and Tyupkin, 1997, 1999; Huang and Sobolev, 2001). We made most of our calculations by taking $r_0 = 50$ km and $t_0 = 1$ year, although we also made the calculations by changing the characteristic distance, r_0 and the characteristic time-span, t_0. The focal depth, $d_i \leq d_0 = 100$ km was chosen as another criterion, although we also made the calculations for the case of $d_i \leq d_0 = 30$ km in this study. The criterion of focal depth is somewhat arbitrary. However, as to be discussed later, this criterion makes little influence to our results.

If we assume that the characteristics of the seismic quiescence at a certain place can be quantified by the minimum RTL value within the investigated period of time, ΔT at this place, we can obtain the spatial distribution of the seismic quiescence by changing the calculated place. A sketch description of this approach is shown in Fig. 1. In this study, we change the place along longitude and latitude at a step of 0.25°. It should be noted that the calculation of the RTL parameter at each place is made through the whole background period, T_{bk}, although we take into account the minimum RTL value only within the study interval, ΔT (Fig. 1).

2.2. S-parameter (an index of the increase of seismicity)

Another algorithm, which is independent from the RTL algorithm, was developed to reveal the spatial distribution of anomaly of seismic activation. We made a simple assumption that the rupture area, S_i of the ith event with magnitude M_i is proportional to $E_i^{2/3}$, where E_i is the seismic energy estimated by the following empirical relation (Kasahara, 1981),

$$\log E_i(\mathrm{J}) = 1.5M_i + 4.8 \tag{3}$$

For convenience, we defined the effective rupture area, S_{eff} as

$$S_{eff} = \frac{1}{\Delta T}\sum_i \frac{S_i}{S_{ref}} = \frac{1}{\Delta T}\sum_i 10^{(M_i - M_{ref})} \tag{4}$$

where ΔT is the time interval of interest and S_{ref} is the rupture area corresponding to a reference magnitude, M_{ref}. A tentative reference magnitude of $M_{ref} = 5$ was used in this study, for the simplicity of calculation. Note that M_{ref} is introduced to normalize the calculation only and makes no influence to the result. The increase of the effective rupture area during a certain time interval, ΔT compared to the averaged background during the background period, T_{bk} (see Fig. 1) would be an index describing the activation level of seismicity. In this study, $\Delta S_{eff} = S_{eff} - S_{bk}$ was chosen as a parameter of the seismic activation, where S_{eff} is the effective rupture area in an investigated activation period, ΔT and S_{bk} is the averaged background one, which can be calculated by Eq. (4) after replacing ΔT by the period of background, T_{bk}.

3. Data analysis

We analyze the JMA earthquake catalog before applying the RTL algorithm. Because the manual operation of data in JMA earthquake catalog has been replaced by the computer operation since 1961, we chose the earthquake catalog from 1961 to 1995 in this study.

At the first step, we eliminate aftershocks from the above JMA catalog using the program written by Smirnov (1998) on the basis of the algorithm of

Molchan and Dmitrieva (1991). The principle of separating aftershocks from the rest of events, which are called background, is based on the comparison of their functions and their distribution in time and space. Background events are assumed to be distributed evenly. Aftershocks are assumed to have a bell-shaped (Gaussian) distribution on the plane (only earthquakes epicenters are taken into account) and are distributed in time according to the Omori law. The parameters of those distributions are estimated iteratively as aftershocks are separated. As a criterion on the basis of which an event is referred to a background events group or to aftershocks the requirement of equal probabilities of classification errors is applied, i.e. classifying a true aftershock with background events and including a true background event into the aftershock group. Thus the total number of classification errors is minimized and mathematical expectation is achieved of the equality of the number of aftershocks and their actual value. The algorithm efficiency was tested by Smirnov (1998) who compared aftershock sequences obtained from regional catalogs with the use of this algorithm and aftershocks catalogs compiled independently by other authors. The discrepancy of the number of aftershocks obtained is approximately 5%.

After eliminating aftershocks from the JMA earthquake catalog, we evaluate the completeness of this catalog using the algorithm developed by Smirnov (1998). For readers' convenience, we introduce briefly the principle of this algorithm as follows.

The evaluation of the completeness of earthquake catalog is based on the histograms of earthquake distribution by magnitude. The problem is to find the minimal value $M_{\min}$ with which the recurrence plot is linear in the range of $M \geq M_{\min}$. To solve this problem, all increasing values of $M_{\min}$ are sorted out. The step of sorting out of $\delta M_{\min}$ should be commensurable with the magnitude assessment error in the catalog. We assume that $\delta M_{\min} = 0.1$ is a constant step in the program. The initial value $M_{\min} = M_{\min 0}$ may be reasonably arbitrary but it should not exceed the magnitude which is associated with the distribution histogram maximum.

First, the hypothesis is tested of the rectilinear character of the empirical recurrence plot. This test is based on the verification of the hypothesis of the agreement of the empirical distribution of earthquakes by magnitudes presented by histogram with the theoretical distribution based on the Gutenberg–Richter relation. If the hypothesis of agreement is accepted on the selected level of significance, $M_{\min}$ is the required assessment of the representative magnitude (i.e. the cut-off magnitude for a complete catalog). In this case, the procedure is over.

The deviation of the recurrence plot from a straight line can be determined both by a 'bend' on the earlier magnitudes (non-representative character of data) and a full-scale character (the real curvature of the graph due to natural properties of seismological process in the Earth). The nature of the curvature of the plot is defined with the next step of the procedure. First, the parameters of recurrence law in the range of $M \geq M_{\min} + \Delta M$ (ΔM is a step being chosen to obtain output result. In our case, we choose $\Delta M = 0.1$) are estimated using the maximum likelihood method. From those parameters, the number of events N_T is calculated in the range of $[M_{\min}, M_{\min} + \Delta M]$, i.e. the recurrence plot is extrapolated to $M_{\min}$ and this 'theoretical' number of events is compared to the observed number of earthquakes $N_H(M_{\min})$. The condition $N_H(M_{\min}) < N_T$ is tested on the basis of statistics on the selected level of significance. If $N_H(M_{\min}) < N_T$, then the non-representative character of events of magnitude $M_{\min}$ is assumed to have caused the deviation of the plot. In this case, the value of $M_{\min}$ is increased by $\delta M_{\min}$ and the whole procedure is repeated. If the condition $N_H(M_{\min}) < N_T$ is not fulfilled statistically, then the hypothesis is assumed of the full-scale character of the curvature of the recurrence plot. In this case, the procedure is stopped and a corresponding mark is entered into the file.

The above-considered algorithm was realized by Smirnov as a set of programs, which allow making assessments of the representative character of earthquake catalogs in varying time intervals and in desired spatial cells. The application of the algorithm of the completeness assessment to a number of regional catalogs testified to its efficiency (Smirnov, 1998).

Fig. 2A plots the temporal variation of the cut-off magnitude, $M_{\min}$ in a circular zone with a radius of $R_{\max} = 100$ km, and a center at the epicenter of the Kobe earthquake. It showed that $M_{\min}$ decreased with time. This would be due to the improvements/changes of the observing instruments of the JMA seismic stations. Some major changes of the JMA network

were reviewed by Ohtake and Ishikawa (1995). We found that a cut-off magnitude $M_{min} = 3.0$ since 1977 is the representative magnitude for the JMA earthquake catalog.

The spatial distribution of the threshold magnitude, M_{min} was also estimated as shown in Fig. 2B by using the JMA catalog during 1977–1995. We found that $M_{min} = 3.0$ can cover most parts of the Japanese islands.

Therefore, we use all events with the magnitude $M \geq 3.0$ in the JMA catalog during 1977–1995 in this study.

4. Results

We calculated the temporal variations of the RTL parameter (in units of the standard deviation, σ) at the epicenter of the $M = 7.2$ Kobe earthquake based on the earthquakes in the circular zone with a radius of R_{max} in the JMA catalog. The spatial distributions of seismic quiescence and activation were also investigated using the methods introduced before.

Fig. 3 shows the temporal variation of the RTL parameter at (135.04°E, 34.59°N), the epicenter of the Kobe earthquake. This RTL curve is obtained on the basis of the RTL algorithm, which was introduced in Section 3. All events used in above calculations satisfy following criteria, magnitude $M_i \geq 3.0$, focal depth $d_i \leq 100$ km, epicentral distance $r_i \leq R_{max} = 100$ km, and time interval $(t - t_i) \leq T_{max} = 2$ years. An obvious seismic quiescence was obtained from this RTL curve, followed by a significant activation stage. The quiescence started in 1993 and reached its bottom one year later. The biggest deviation from the background was about 7σ. The temporal variations of three functions, R(135.04°E, 34.59°N, 0, t), T(135.04°E, 34.59°N, 0, t), and L(135.04°E, 34.59°N, 0, t) are also shown in Fig. 3 with grey lines. These three functions deviate consistently from their background levels in 1994.

The spatial distribution of the seismic quiescence is plotted in Fig. 4. We calculated the quiescence distribution during May 11, 1993–May 10, 1994, because a significant quiescence stage was revealed during this period by the RTL parameter (Fig. 3). An anomaly of quiescence appeared around the epicenter of the Kobe earthquake. The linear dimension of this anomalous zone was about 300 km. Some other quiescence anomalies are also detected during the same investigated period. However, as we will discuss in Section 5, we cannot ensure the reliability of these anomalies, although there is a possibility that some of these anomalies may have some correlation with the nearby earthquakes (Fig. 4).

Fig. 5 shows the spatial distribution of the seismic activation during an interval of seven months from May to December in 1994, because an obvious activation stage was detected during this period by the RTL parameter (Fig. 3). An anomalous zone of seismic activation in order of several tens of kilometers was obtained around the epicenter of the Kobe earthquake.

5. Discussion

5.1. RTL anomaly and quality of earthquake data

The seismic quiescence of the Kobe earthquake started in 1993 and lasted till May 1994, about eight months before the mainshock (Fig. 3). The duration time was about one year and the biggest deviation from the background level was -6.94σ. The distance function R(135.04°E, 34.59°N, 0, t), time function T(135.04°E, 34.59°N, 0, t), and rupture length L(135.04°E, 34.59°N, 0, t) decreased consistently from their background levels during 1993–1994 (Fig. 3). As mentioned in Section 4, these three functions are normalized by their standard deviations, σ_R, σ_T, and σ_L, respectively. It would be possible to estimate roughly the probability of these variations. The values of these three functions at the time when the RTL parameter has the biggest deviation in May 1994 are $-1.54\sigma_R$, $-1.98\sigma_T$, and $-2.27\sigma_L$, respectively. After assuming a normal distribution, the occurrence probabilities of above anomalies are 0.123, 0.0478, and 0.0232, respectively. If these three functions are completely independent, the occurrence probability of above RTL anomaly in May 1994 would be 1.4×10^{-5}.

Besides the anomaly in 1994, another RTL anomaly was also detected in 1984 (Fig. 3). In fact, during the analyzed time window from 1977 to 1995, there occurred another two moderate earthquakes with $M >$ 5.5 in the study zone. The occurrence time of these

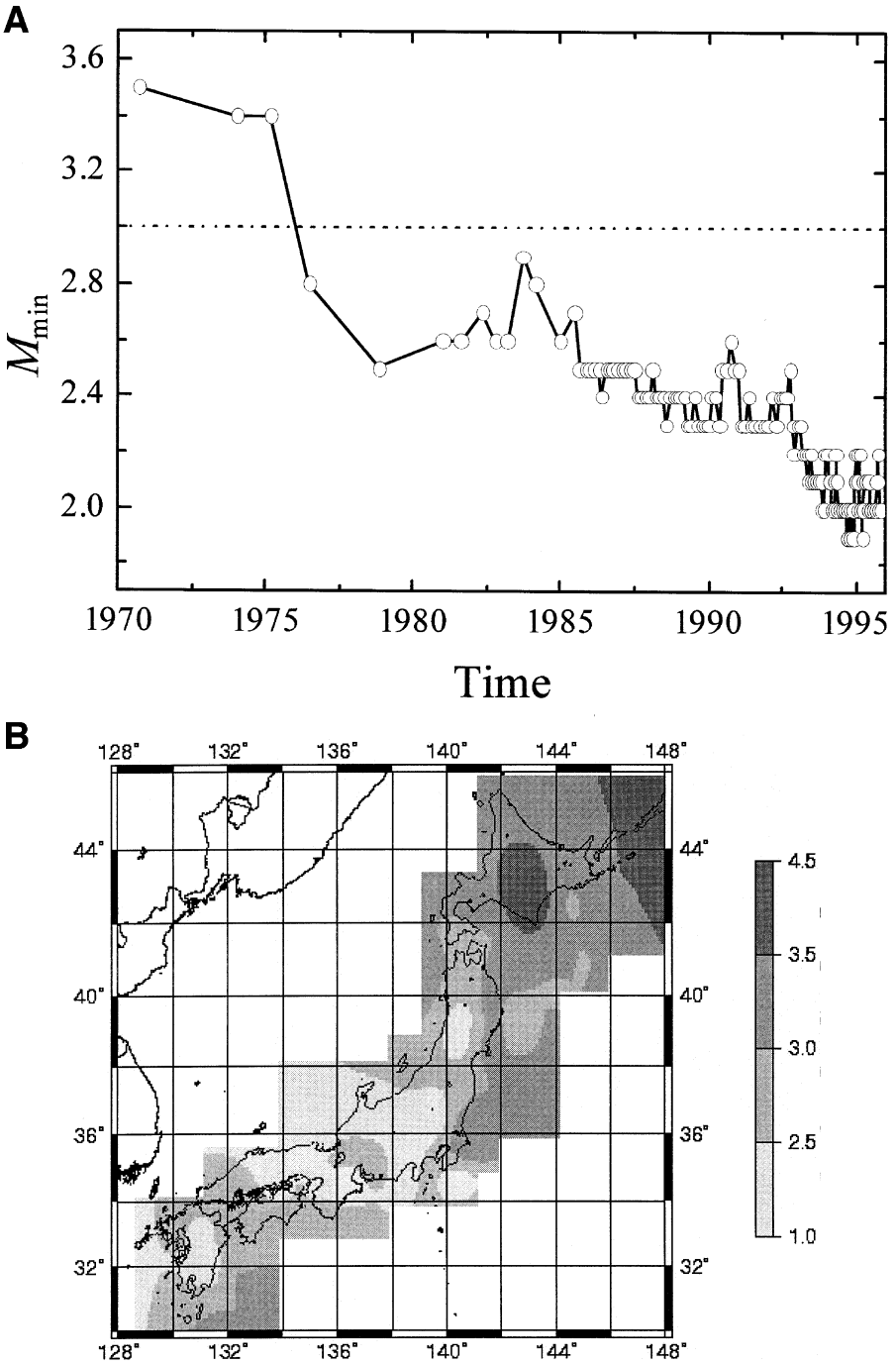

Fig. 2. The minimum magnitude, M_{min} for the completeness of the JMA catalog. (A) Temporal variation in the zone within 100 km around the epicenter of the $M = 7.2$ Kobe (Japan) earthquake, January 17, 1995. (B) Spatial distribution of M_{min}. The shadowed zone indicates the calculated region in this study.

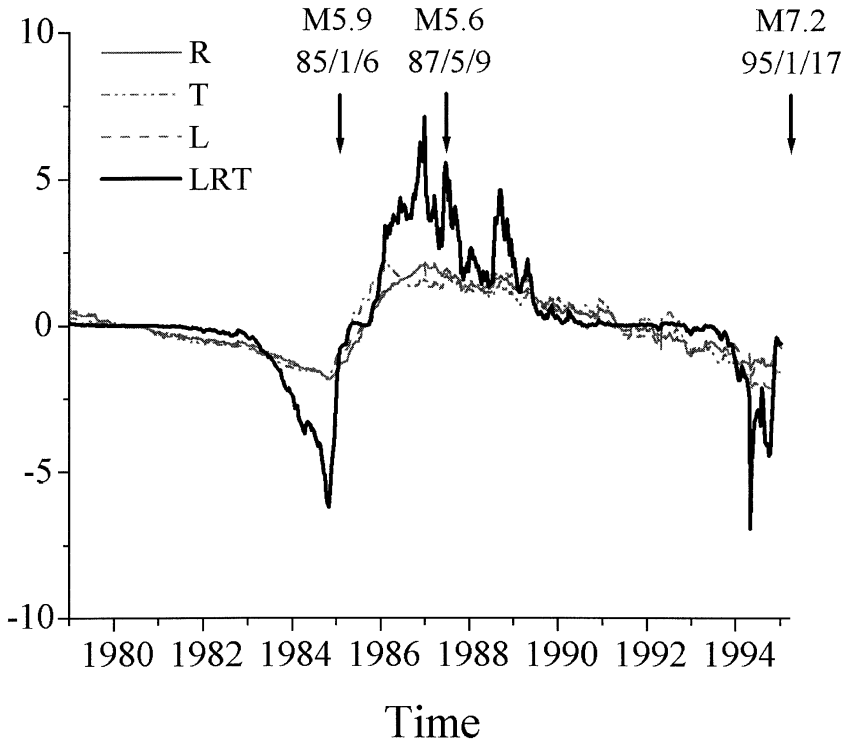

Fig. 3. The temporal variation of the RTL parameter at (135.04°E, 34.59°N), the epicenter of the 1995 Kobe earthquake. This curve is obtained by changing the calculated time at a step of 10 days. A significant quiescence appeared in 1993, followed by an activation stage. Arrows indicated the occurrence time of earthquakes. The $M = 5.9$ earthquake occurred on January 6, 1985 and the $M = 5.6$ earthquake occurred on May 9, 1987.

two events is also shown in Fig. 3. Namely, an $M = 5.9$ earthquake occurred on January 6, 1985 and an $M = 5.6$ earthquake occurred on May 9, 1987. Unfortunately, it is not clear whether the anomaly around 1985 was associated with the preparation of these earthquakes or not, because it is not easy to judge the influence of the changes of the JMA seismological network during this period.

Generally, seismicity changes have two possible causes: (1) the real changes associated with the preparation of earthquakes; (2) the artificial effect due to the changes of seismological networks (Habermann, 1987, 1991). In order to differentiate the RTL anomalies between above two possibilities, we evaluate the quality of the JMA data and discuss the possible causes of the RTL anomalies that are obtained in this study.

We investigate the temporal variations of the earthquake number in the study zone ($r_i \leq R_{\max} = 100$ km). There are total 14825 events that occurred in the study zone during 1977–1995. The histogram of yearly number and the diagram of cumulative number are shown in Fig. 6A and B, respectively. There are significant increases of earthquake number around 1984 and around 1993–1995. These increases may be due to the changes of the JMA seismic network.

In fact, the JMA network has undergone many changes not only in the instrumentation but also in data management. Some major changes of the nation-wide JMA network till 1990 was discussed by Ohtake and Ishikawa (1995). The JMA improved the accuracy of locating focal depth, longitude and latitude in October 1983. The JMA network of Osaka local center (including the Kobe region) introduced the new system of L/ADESS (local automated

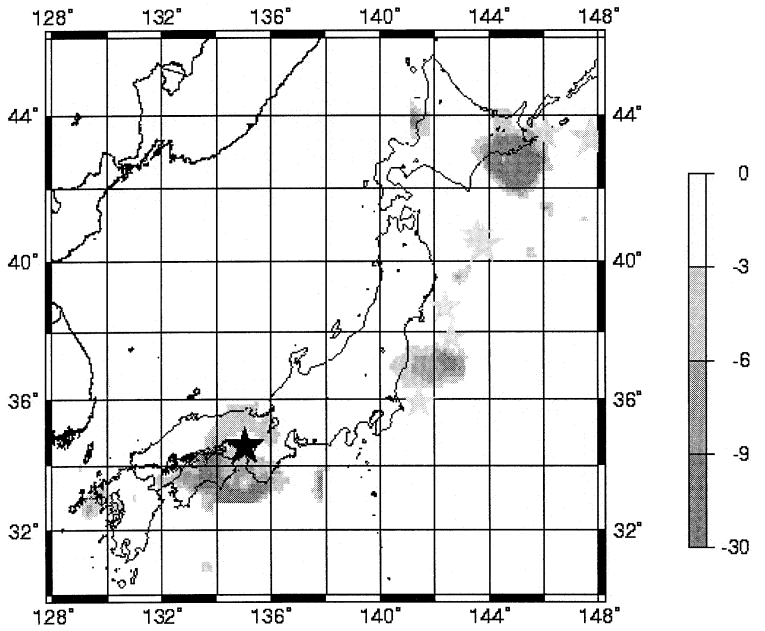

Fig. 4. A significant seismic quiescence appeared during May 1993–May 1994. The anomalous zone reached 300 km. The scale on the right corresponds to the RTL value in the unit of the standard deviation. The black star represents the epicenter of the Kobe earthquake (135.04°E, 34.59°N). The grey stars indicate the epicenters of earthquakes with $M \geq 6.0$ during June 1, 1994–December 31, 1995 (see Table 1).

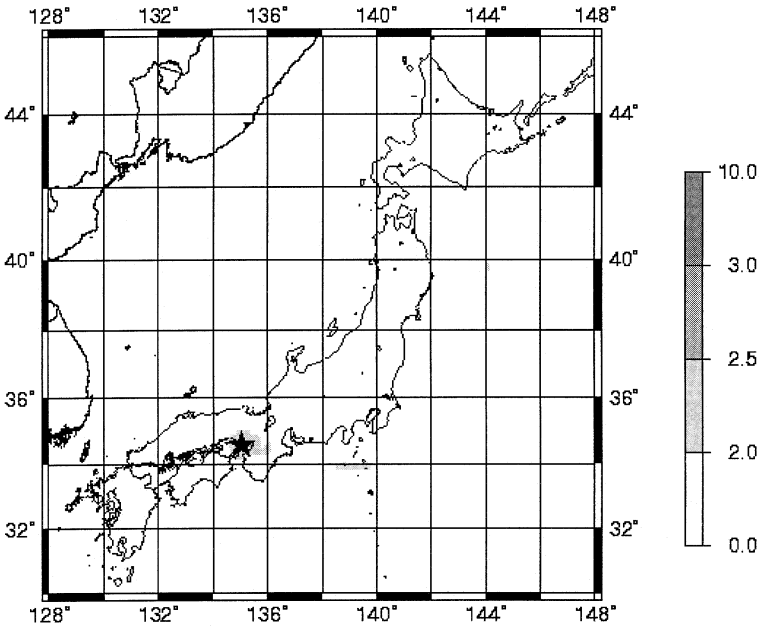

Fig. 5. Spatial distribution of seismic activation during May–December 1994. The epicenter of the Kobe earthquake (black star) located almost in the center of this anomalous zone, which is in order of several tens of kilometers.

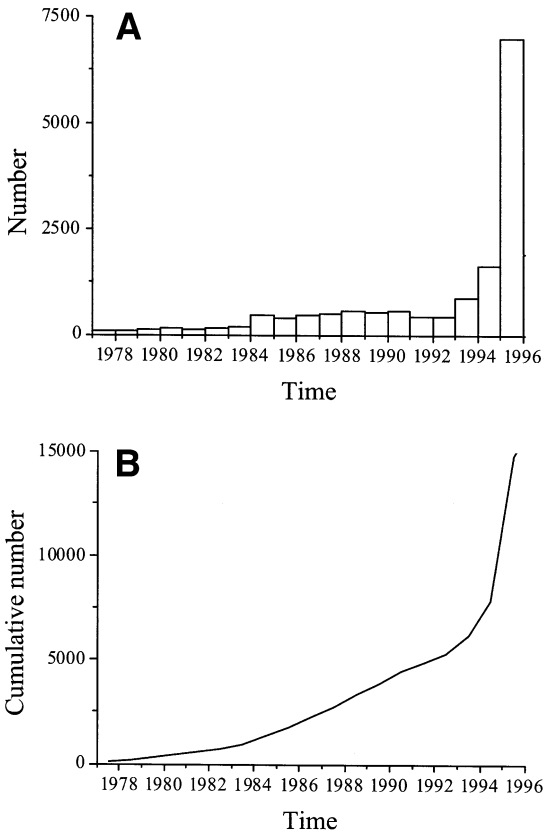

Fig. 6. The temporal variation of the number of earthquakes during 1977–1995 in a circular zone within 100 km from the epicenter of the 1995 Kobe earthquake. (A) Histogram of yearly number. (B) Cumulative number.

data editing and switching system) in 1984. The above changes of data observing and processing systems of the JMA Osaka local center would explain the sudden increase of earthquake number around 1984. Besides above changes, the system of ETOS (earthquake and tsunami observation system) has been introduced in the JMA stations of Osaka local center since 1993 and the temporary tsunami observation network was on operation from October 1994 to early 1995. The significant increase of earthquake number during 1993–1995 may be associated with the above changes of the JMA network of Osaka local center.

After the procedure of aftershock elimination, 5056 events (about 34% of the total events) are identified as aftershocks and thus are eliminated from the catalog. For comparison, we plot the diagrams of cumulative number with $M_i \geq 3.0$ before and after the application of aftershock elimination algorithm in Fig. 7A and B, respectively. It is clear that most aftershocks are eliminated by the algorithm we applied. After comparing Fig. 6B with Fig. 7B, we found that the influence due to the changes of the JMA seismic network during 1993–1995 can be reduced significantly after introducing a cut-off magnitude $M_{\min} = 3.0$ and eliminating aftershocks from the earthquake catalog. Therefore, the quiescence anomaly in 1994 (Fig. 3), which was revealed by the RTL algorithm, would have reasonable correlation with the preparation of the $M = 7.2$ Kobe earthquake. As mentioned before, another significant RTL anomaly was detected in 1984 and two moderate earthquakes occurred in the study zone. Although there is a possibility that the anomaly in 1984 is associated with the followed events, it is also possible that this anomaly is an artificial effect due to the changes of the JMA seismological network (Fig. 7A).

5.2. Influence of d_0, r_0 and t_0

As mentioned in Section 2.1, we introduced some 'free' parameters such as cut-off focal depth d_0, characteristic distance r_0, and characteristic time-span t_0. We chose these parameter as $d_0 = 100$ km, $r_0 = 50$ km ($R_{\max} = 2r_0 = 100$ km) and $t_0 = 1$ year ($T_{\max} = 2t_0 = 2$ years) in our above calculations. Although the criterion of d_0 is somewhat arbitrary, the criteria of r_0 and t_0 are chosen not only on the basis of our previous experiences, but also on the basis of the reports of rupture region and duration time of seismic quiescence. In order to investigate the possible influence to the results, we repeat our calculations by changing these parameters. For simplification, we plot the RTL curves after changing only one parameter at each case. We also calculate the correlation coefficient between the previous result (Fig. 3) and the result we obtained at each case (Figs. 8–10).

First, we discuss the influence of the cut-off focal depth d_0, which is somewhat arbitrary in this study. We re-calculated the RTL parameter after replacing $d_0 = 100$ km by $d_0 = 999$ km (this depth is deep enough to cover the depth range of all earthquakes) and $d_0 = 30$ km (this is a typical threshold depth of earthquakes in crust), respectively and keeping other

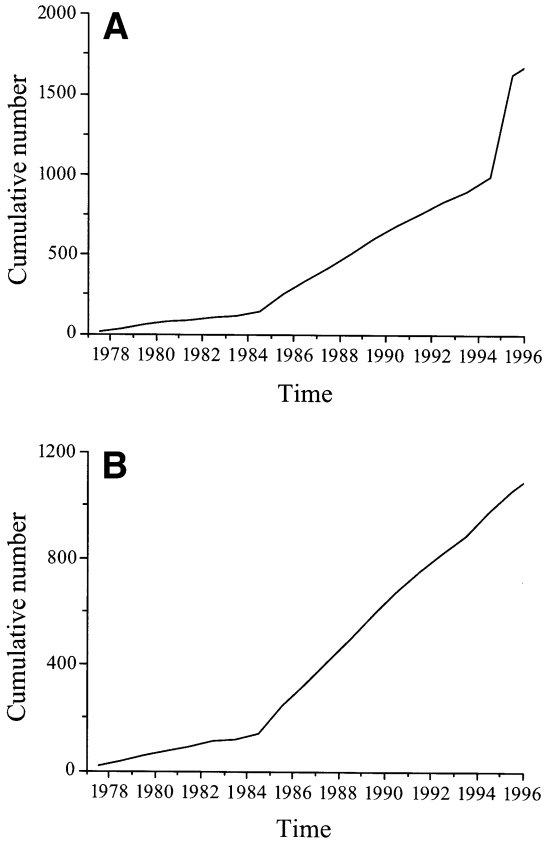

Fig. 7. The temporal variation of the number of earthquakes during 1977–1995 satisfying $M \geq 3.0$ in a circular zone within 100 km from the epicenter of the 1995 Kobe earthquake. (A) Before eliminating aftershocks. (B) After eliminating aftershocks.

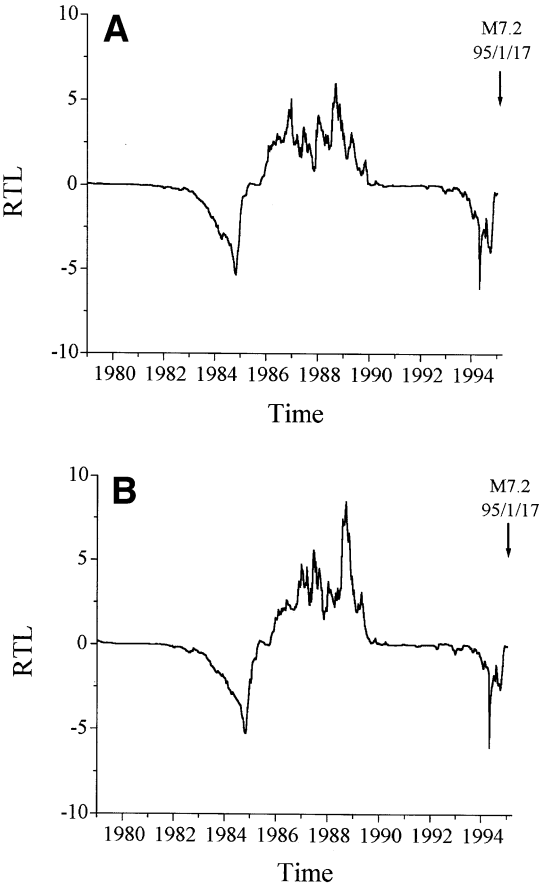

Fig. 8. The temporal variation of the RTL parameter at the epicenter of the 1995 Kobe earthquake. We keep $r_0 = 50$ km ($R_{max} = 2r_0 = 100$ km) and $t_0 = 1$ year ($T_{max} = 2t_0 = 2$ years) in both cases. (A) $d_0 = 999$ km. (B) $d_0 = 30$ km.

parameters unchanged (i.e. $r_0 = 50$ km and $t_0 = 1$ year). The relevant results are plotted in Fig. 8A and B, respectively. We found that there is little influence to the RTL parameter from the changes of the cut-off focal depth d_0. We also estimated the correlation coefficient between the cases between $d_0 = 100$ and $d_0 = 999$ km and between $d_0 = 100$ and $d_0 = 30$ km. We obtained the correlation coefficients of 0.960 and 0.926 for above two cases (see Table 1). The statistic test indicated that significant correlation exists for above both cases at a significant level of 0.05 (Bendat and Piersol, 2000). Namely, the changes

Table 1
Correlation of RTL values between different model parameters ($R_{max} = 2r_0$ and $T_{max} = 2t_0$)

Cases	A	$d_0 = 100$ km, $r_0 = 50$ km, $t_0 = 1$ year					
	B	$d_0 = 999$ km, $r_0 = 50$ km, $t_0 = 1$ year	$d_0 = 30$ km, $r_0 = 50$ km, $t_0 = 1$ year	$d_0 = 100$ km, $r_0 = 25$ km, $t_0 = 1$ year	$d_0 = 100$ km, $r_0 = 75$ km, $t_0 = 1$ year	$d_0 = 100$ km, $r_0 = 50$ km, $t_0 = 0.5$ year	$d_0 = 100$ km, $r_0 = 50$ km, $t_0 = 1.5$ years
Correlation coefficient		0.960	0.926	0.861	0.981	0.632	0.731

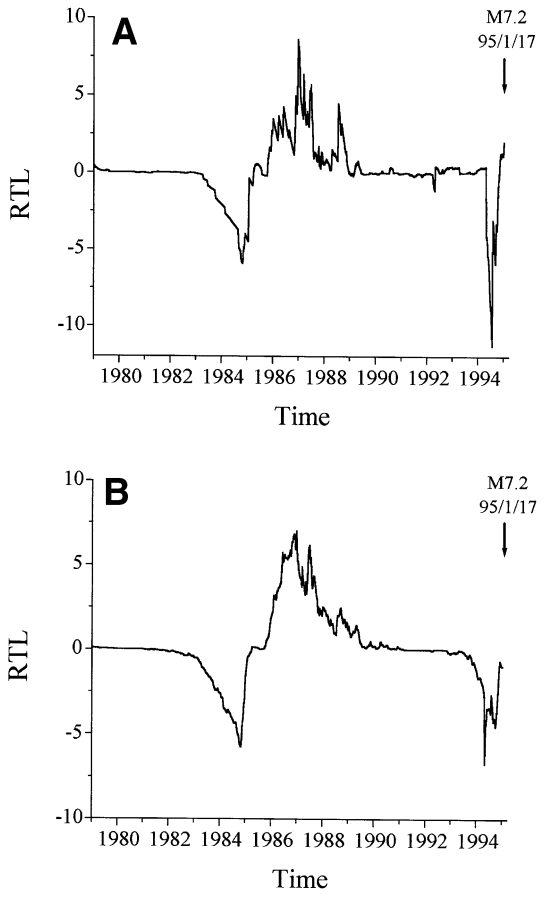

Fig. 9. The temporal variation of the RTL parameter at the epicenter of the 1995 Kobe earthquake. We keep $d_0 = 100$ km and $t_0 = 1$ year ($T_{max} = 2t_0 = 2$ years) in both cases. (A) $r_0 = 25$ km ($R_{max} = 2r_0 = 50$ km). (B) $r_0 = 75$ km ($R_{max} = 2r_0 = 150$ km).

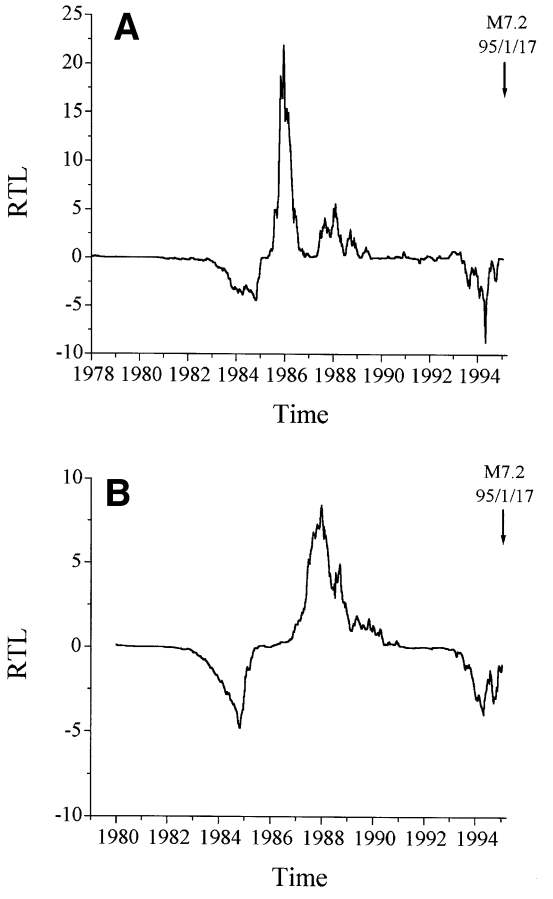

Fig. 10. The temporal variation of the RTL parameter at the epicenter of the 1995 Kobe earthquake. We keep $d_0 = 100$ km and $r_0 = 50$ km ($R_{max} = 2r_0 = 100$ km) in both cases. (A) $t_0 = 0.5$ year ($T_{max} = 2t_0 = 1$ year). (B) $t_0 = 1.5$ years ($T_{max} = 2t_0 = 3$ years).

of the cut-off focal depth d_0 do not influence much to our results.

Next, we investigate the influence of the characteristic distance r_0. Fig. 9A and B shows the temporal variations of RTL parameter in case of $r_0 = 25$ km ($R_{max} = 2r_0 = 50$ km) and $r_0 = 75$ km ($R_{max} = 2r_0 = 150$ km), respectively (we keep other parameters unchanged, i.e. $d_0 = 100$ km and $t_0 = 1$ year). In both cases, we obtained quite similar results to the previous one (Fig. 3). The RTL anomaly in 1994 is more significant as the investigated region is constricted in a much narrower zone (e.g. $r_0 = 25$ km) around the epicenter of the Kobe earthquake (Fig. 9A). There is no increase of the RTL anomaly around 1984. It seems that the RTL anomaly in 1994 has reasonable correlation with the preparation of the Kobe earthquake. The correlation coefficients are 0.861 and 0.981, respectively for the cases between $r_0 = 25$ and $r_0 = 50$ km and between $r_0 = 75$ and $r_0 = 50$ km (see Table 1). The statistic test indicated that significant correlation exists between the previous result (Fig. 3) and the current results (Fig. 9A and B) at a significant level of 0.05.

Finally, we estimate the influence of the characteristic time-span t_0. We repeat the calculations by changing t_0 from 1 to 0.5 year ($T_{max} = 2t_0 = 1$ year) and 1.5 years ($T_{max} = 2t_0 = 3$ years) and keeping other parameters unchanged (i.e. $d_0 = 100$ km and

Table 2
List of earthquakes satisfying following criteria: magnitude, $M \geq 6.0$, focal depth, $d \leq 100$ km, and time window, June 1, 1994–December 31, 1995

Date (local)	Time (local)	Longitude (°E)	Latitude (°N)	Depth (km)	Magnitude (JMA)
940814	18:06:50	142.39	38.68	42	6.0
940816	19:09:32	142.6	37.83	22	6.0
940831	18:07:29	146.07	43.49	84	6.5
941004	22:22:56	147.71	43.37	23	8.1
941228	21:19:20	143.75	40.43	0	7.5
950110	03:00:18	141.43	35.93	43	6.1
950117	05:46:51	135.04	34.59	18	7.2
951230	21:17:34	143.55	40.72	0	6.1

$r_0 = 50$ km). The temporal variations of RTL values of above two cases are plotted in Fig. 10A and B, respectively. Similar characteristics of seismicity changes are obtained. There is a tendency that the narrower the time-span is, the more significant the RTL anomaly in 1994 would be. The correlation coefficients are 0.632 and 0.731, respectively, for above two cases (see Table 1). Both cases (Fig. 10A and B) have a significant correlation with our previous result (Fig. 3) at a significant level of 0.05.

We also repeat the calculations by keeping the cut-off focal depth $d_0 = 30$ km and changing the characteristic distance r_0 and/or the characteristic time-span t_0. Still we obtained the same conclusion that there is significant correlation between the previous result in Fig. 3 and any case we investigated at a significant level of 0.05.

Even we change simultaneously two or three parameters of d_0, r_0 and t_0, we found that these results have significant correlation with the previous result at a significant level of 0.05.

Above analyses indicate that the RTL result we obtained previously in Fig. 3 is unlikely an artificial effect due to the selection of some model parameters, d_0, r_0 and t_0. Therefore, we can conclude reasonably that the RTL anomaly, which appeared in 1994, would correlate with the preparing of the $M = 7.2$ Kobe earthquake.

5.3. Temporal evolution of spatial distributions of seismic quiescence and activation

The spatial distribution of seismic quiescence during this period indicated that the linear size of this anomalous zone is nearly 300 km (Fig. 4), several times larger than the rupture length, which is in order of several tens of kilometers. Besides the quiescence anomaly around the epicentral zone of the Kobe earthquake, other anomalies of quiescence were also obtained during the same period. In order to investigate the possible correlation between these anomalies and earthquakes, all mainshocks with $M \geq 6.0$ during June 1, 1994–December 31, 1995 are listed in Table 2. These earthquakes are also marked by stars in Fig. 4. It seems that the anomalies in Kanto and Hokkaido areas have some correlation with the nearby earthquakes. However, these two zones did not locate in the area with $M_{\min} = 3.0$, considering the spatial distribution of the cut-off magnitude (Fig. 2B). Namely, the completeness of the JMA catalog in these two zones cannot be satisfied, because a constant $M_{\min} = 3.0$ was chosen in our calculations. Therefore, we do not take these anomalies into account because we cannot ensure the reliability. On the other hand, we cannot deny the possibility of the existence of some correlation between the anomalous zones and the nearby events, because we did not make detailed investigations for these earthquakes by choosing another cut-off magnitude, which ensures the completeness of earthquake catalog in that/those zone(s). At current stage, we can only conclude that the anomaly around epicenter during May 1993–May 1994 is a reliable and significant anomaly of quiescence before the Kobe event.

The activation stage appeared in May 1994 with a duration of about seven months. A significant anomalous activation zone in order of several tens kilometer was detected during May–December 1994

(Fig. 5). The epicenter located almost in the center of this anomalous zone. This result is consistent with those obtained for the earthquakes in Kamchatka and Hokkaido, although their occurrence time before the mainshocks is somewhat different (Sobolev and Tyupkin, 1997, 1999; Huang and Sobolev, 2001). Therefore, the anomalous activation zone obtained by the algorithm in this study may provide some detailed information on locating the future risk regions.

We also calculated the spatial distributions of quiescence and activation for different time window, to investigate their evolution characteristics and the possible correlation between the anomalous quiescence/activation zone and the Kobe earthquake. Fig. 11A gives the quiescence map during May 1992–May 1993. No clear quiescence was detected around the epicentral zone of the $M = 7.2$ Kobe earthquake. It seems that the quiescence stage did not start during this period. This result is consistent with that observed by the RTL parameter (Fig. 3). The quiescence map on January 17, 1995 is given in Fig. 11B. The previous anomaly during 1993–1994 (see Fig. 4) disappeared. It is suggested that the evolution of seismic quiescence revealed by the RTL algorithm has a plausible correlation with the seismogenic process of the 1995 Kobe earthquake.

Fig. 12A shows the activation map in 1993. No clear activation was observed in the epicentral zone of the Kobe event, consistent with the result revealed by the RTL parameter (Fig. 3). It should be mentioned that an intense activation anomaly was detected around the Izu Peninsula of the Tokai area (Fig. 12A). The activation anomaly, which was detected during May–December 1994, disappeared after the occurrence of the Kobe earthquake (see Fig. 12B). Again, a significant activation anomaly was obtained around the Izu Peninsula. Unfortunately, no any strong earthquake occurred after the above anomalies in 1993 and 1995. We checked the seismicity of the Izu Peninsula and found that there were many earthquake swarms around the Izu area during 1993–1998 (Earthquake Prediction Information Division, Japan Meteorological Agency, 1999). At current stage, the correlation of the above activation anomalies in the Izu area and these earthquake swarms is still unknown. Further study on the seismicity changes of swarms would be interesting, but it is out of the scope of this paper. The evolution of activation zone in different time interval suggests that the activation anomaly, which appeared around the epicentral zone during May–December 1994, would have some reasonable correlation with the Kobe event.

We also investigated the spatial distribution of seismic quiescence and activation based on the cut-off focal depth $d_0 = 30$ km and obtained quite similar results.

The temporal variation of the seismicity changes of the 1995 Kobe earthquake revealed by the RTL algorithm showed similar characteristics to those obtained from some strong earthquakes in Kamchatka (Sobolev and Tyupkin, 1997, 1999) and the $M = 6.8$ Nemuro Peninsula earthquake in Hokkaido (Huang and Sobolev, 2001). The seismic quiescence stages started 1.5–3.5 years before the mainshock and lasted 1–2.5 years. The subsequent stages of seismic activation had a duration varying from 0.5 to 1.5 years. The seismic quiescence anomalies appear in a broad zone several times larger than the rupture length of the mainshock and the activation zones are comparable to the rupture length.

The similar variations of seismicity changes prior to strong earthquakes in different tectonic regions may reflect the natural evolution of seismogenic process. Tests in Russia and Japan indicated that the RTL algorithm is an effective tool for revealing the seismic quiescence and activation patterns before strong earthquakes.

6. Conclusion

We investigated seismicity changes of quiescence and activation patterns prior to the $M = 7.2$ Kobe (Japan) earthquake, January 17, 1995 by applying the RTL algorithm to the earthquake catalog of the JMA. The mainshock occurred after the completion of the quiescence and activation stages. After evaluating the data quality and the influence of the changes of some model parameters, we conclude that the quiescence anomaly in 1994, which was revealed by the RTL parameter, has a reliable correlation with the preparation of the Kobe earthquake. The maximum linear size of the anomalous quiescence zone during May 1993–May 1994 was several times larger than the rupture length of the mainshock. An anomalous

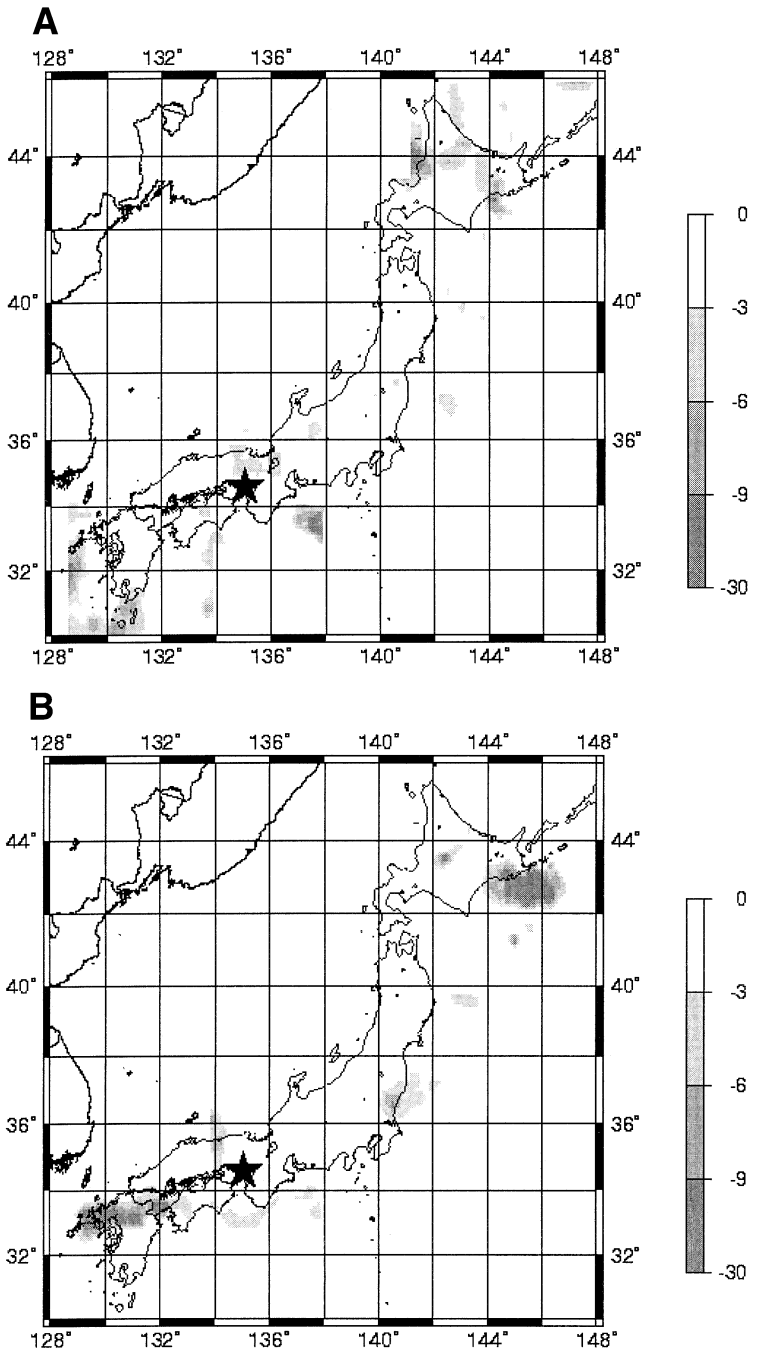

Fig. 11. Spatial distribution of seismic quiescence. (A) During May 1992–May 1993; (B) on January 17, 1995. No significant quiescence anomaly appeared around the epicentral zone for both cases.

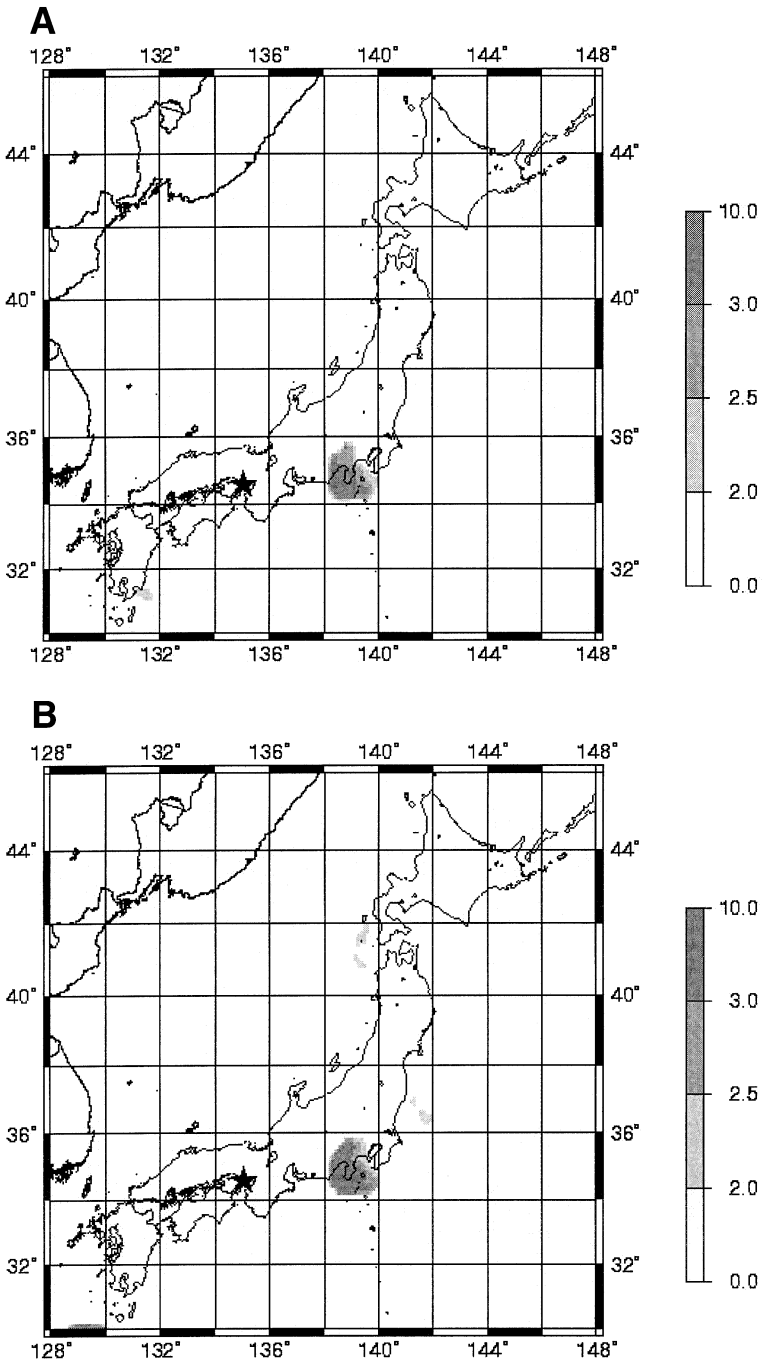

Fig. 12. Activation map in (A) 1993; (B) 1995. No significant anomaly appeared around the epicenter.

zone of activation in order of several tens of kilometers appeared around the epicenter after the quiescence stage. The epicenter of the coming mainshock was almost in the center of this anomalous zone. Such activation anomaly detected after a quiescence pattern may provide useful information for locating the future risk zones. Investigations of the evolution of spatial distribution of seismic quiescence indicated that no quiescence anomaly appeared in the epicentral zone during May 1992–May 1993. The quiescence anomaly around the Kobe area during May 1993–May 1994 disappeared after the occurrence of the mainshock. We obtained similar characteristics of the evolution of spatial distribution of seismic activation around the Kobe region. Namely, no activation anomaly appeared before (e.g. in 1993) and after (e.g. in 1995) the activation stage around the epicentral zone. Therefore, there would have reasonable correlation between the seismicity changes around the Kobe region and the preparation of the Kobe earthquake.

Acknowledgements

The authors thank the Japan Meteorological Agency (JMA) for providing the earthquake catalog and V.B. Smirnov for offering the programs of removing aftershocks and estimating threshold magnitude of a complete catalog. The authors also thank Dr Y. Ishikawa for providing information of the changes of the JMA network. This study is supported by the Frontier Research System of RIKEN (The Institute of Physical and Chemical Research), Japan.

References

Bendat, J.S., Piersol, A.G., 2000. Random Data: Analysis and Measurement Procedures. Wiley, New York, 594 pp.

Bowman, D.D., Ouillon, G., Sammis, C.G., Sornette, A., Sornette, D., 1998. An observational test of the critical earthquake concept. J. Geophys. Res. 103, 24359–24372.

Earthquake Prediction Information Division, Japan Meteorological Agency, 1999. Seismicity in Izu Peninsula and its surrounding area. Report of the coordinating committee for earthquake prediction, Japan, 61, 218–221 (in Japanese).

Habermann, R.E., 1987. Man-made changes in seismicity rates. Bull. Seismol. Soc. Am. 77, 141–159.

Habermann, R.E., 1988. Precursory seismic quiescence: past, present, and future. Pure Appl. Geophys. 126, 279–318.

Habermann, R.E., 1991. Seismicity rate variations and systematic changes in magnitudes in teleseismic catalogs. In: Wyss, M. (Ed.), Earthquake Prediction. Tectonophysics 193, 277–289.

Huang, Q., Sobolev, G.A., 2001. Seismic quiescence prior to the 2000 $M = 6.8$ Nemuro Peninsula earthquake. Proc. J. Acad. 77, 1–6.

Ishikawa, Y., 1990. Inland seismic gaps of the Japanese islands. Earth Monthly 12, 355–362 (in Japanese).

Kasahara, K., 1981. Earthquake Mechanics. Cambridge University Press, Cambridge, 248 pp.

Katsumata, K., Kasahara, M., 1999. Precursory seismic quiescence before the 1994 Kurile earthquake ($M_w = 8.3$) revealed by three independent seismic catalogs. Pure Appl. Geophys. 155, 443–470.

Keilis-Borok, V.I., Kossobokov, V.G., 1990. Premonitory activation of seismic flow: algorithm M8. Phys. Earth Planet. Inter. 61, 73–83.

Kossobokov, V.G., Keilis-Borok, V.I., 1990. Localization of intermediate-term earthquake prediction. J. Geophys. Res. 95, 763–772.

Mjachkin, V.I., Brace, W.F., Sobolev, G.A., Dieterich, J.H., 1975. Two models for earthquake forerunners. Pure Appl. Geophys. 113, 169–181.

Mogi, K., 1968. Source locations of elastic shocks in the fracturing process in rocks (1). Bull. Earthquake Res. Inst. 46, 1103–1125.

Mogi, K., 1979. Two kinds of seismic gaps. Pure Appl. Geophys. 117, 1172–1186.

Molchan, G.M., Dmitrieva, O.E., 1991. Identification of aftershocks: review and new approaches. Comput. Seismol. 24, 19–50 (in Russian).

Ohtake, M., Ishikawa, Y., 1995. Seismic observation networks in Japan. J. Phys. Earth 43, 563–584.

Scholz, C.H., 1968. Experimental study of the fracturing process in brittle rock. J. Geophys. Res. 73, 1447–1454.

Smirnov, V.B., 1998. Earthquake catalogs: Evaluation of data completeness. Volcanol. Seismol. 19, 433–446.

Sobolev, G.A., 1995. Fundamental of Earthquake Prediction. Electromagnetic Research Centre, Moscow, 162 pp.

Sobolev, G.A., Tyupkin, Y.S., 1997. Low-seismicity precursors of large earthquakes in Kamchatka. Volcanol. Seismol. 18, 433–446.

Sobolev, G.A., Tyupkin, Y.S., 1999. Precursory phases seismicity precursors, and earthquake prediction in Kamchatka. Volcanol. Seismol. 20, 615–627.

Sornette, D., Sammis, C.G., 1995. Complex critical exponents from renormalization group theory of earthquakes: implication for earthquake prediction. J. Phys. 5, 607–619.

Takanami, T., Sacks, I.S., Snoke, J.A., Motoya, Y., Ichiyanagi, M., 1996. Seismic quiescence before the Hokkaido-Toho-Oki earthquake of October 4, 1994. J. Phys. Earth 44, 193–203.

Taylor, D.W.A., Snoke, J.A., Sacks, I.S., Takanami, T., 1991.

Seismic quiescence before the Urakawa-Oki earthquake. Bull. Seismol. Soc. Am. 81, 1255–1271.

Varnes, D.J., 1989. Predicting earthquakes by analyzing accelerating precursory seismic activity. Pure Appl. Geophys. 130, 661–686.

Wiemer, S., Wyss, M., 1994. Seismic quiescence before the Landers ($M = 7.5$) and Big Bear ($M = 6.5$) 1992 earthquakes. Bull. Seismol. Soc. Am. 84, 900–916.

Wyss, M., Habermann, R.E., 1988. Precursory seismic quiescence. Pure Appl. Geophys. 126, 319–332.

Wyss, M., Habermann, R.E., Griesser, J.C., 1984. Seismic quiescence and asperities in the Tonga-Kermadec Arc. J. Geophys. Res. 89, 9293–9304.